DEVELOPMENT OF NON-INVASIVE CALIBRATION SOFTWARE FOR FRONT END X-RAY BEAM POSITION MONITORS AT DIAMOND LIGHT SOURCE

C. Houghton*, C. Bloomer, L. Bobb, Diamond Light Source Ltd, United Kingdom

Abstract

Tungsten blade based photoemission X-ray Beam Position Monitors (XBPMs) are widely used as white beam diagnostics at synchrotrons. Traditionally, the scale factors are determined by stepper motor movements of the XBPM, or by controlled electron beam displacements, and measuring the response. These measurements must be repeated for each ID gap to produce a complete set of scale factors for all operational conditions. This calibration procedure takes time and cannot be done while users are acquiring data. In addition, the scale factors can vary over time due to changes to the storage ring. It is possible for these scale factors to become inaccurate, reducing the accuracy of the beam position measured by the XBPMs. By using the intrinsic kHz electron beam movements and correlating the signals from electron beam position monitors and XBPMs it is possible to have real-time calculation of the scale factors without the need to disturb user operation. Presented in this paper is a method to non-invasively calculate scale factors during normal user operation. A comparison of the precision of this method versus the traditional stepper motor method is presented.

INTRODUCTION

To monitor and improve the stability of the photon beam Diamond Light Source utilises two X-ray beam position monitor (XBPMs) on most insertion device (ID) front ends. Each XBPM is mounted on stepper motors to enable precise alignment of the XBPM with the incident X-ray beam. Traditionally, the XBPM calibration factors, or 'scale factors' are obtained by measuring the position response of the XBPM whilst a known stepper motor offset is applied, to simulate real X-ray beam movements. Alternatively, the beam movements can be generated using an electron beam bump. Corrector magnets are used to induce a known angular offset through the ID. This in turn produces a fixed offset of the X-ray beam at the XBPM. A scale factor, K, can be calculated by comparing the measured response of the four XBPM blades to the known applied beam offset. The response of the XBPM is defined by

$$(\Delta/\Sigma)_x = \frac{(I_A + I_D) - (I_C + I_B)}{I_A + I_B + I_C + I_D} \tag{1a}$$

$$(\Delta/\Sigma)_y = \frac{(I_A + I_B) - (I_C + I_D)}{I_A + I_B + I_C + I_D} \tag{1b}$$

where Δ/Σ is a dimensionless position and $I_{(A,B,C,D)}$ are the currents from the four XBPM blades (A = top-left; B = top-right; C = bottom-right; D = bottom-left) when viewed from the X-ray source. The calculation of the XBPM scale factors using these methods has several limitations. Firstly, both these methods require specific machine development time and cannot be done during user operation. Secondly, the XBPM scale factor is dependent on the ID settings particularly the ID gap. As the ID gap varies there are changes to the XBPM sensitivities due to the change in the photon beam distribution [1, 2]. Currently, the scale factors, K_x and K_y, are calculated for a selection of ID gaps and can be used to convert the dimensionless position, Δ/Σ, to a horizontal and vertical position in millimeters. Current methods for calibration use interpolation in order to populate lookup tables for all possible ID gaps.

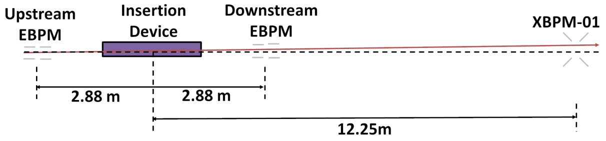

Figure 1: Schematic of the EBPM and XBPM locations for a typical Diamond Light Source Insertion Device straight.

Presented in this paper is a method for utilising the intrinsic electron beam movements and fast electronics in order to calculate XBPM scale factors passively during user operation.

SET-UP

Diamond Light Source has a Fast Acquisition network which can synchronously capture the position data from electron beam position monitors (EBPMs) and XBPMs at a rate of 10 kHz [3]. This data stream allows for the comparison of the electron beam trajectory through the ID with the X-ray beam position at the XBPM. For the duration of one user run at Diamond Light Source, 1 s of the 10 kHz position data was collected from the EBPMs and XBPMs at intervals of 10 seconds from the I14 insertion device beamline. The 'projected' position of the X-ray beam at the XBPM is determined from a geometric projection of the EBPM measurements from either side of the insertion device out to the distance of the XBPM. Figure 1 shows a schematic of the system and distance to these components.

The projected and measured X-ray beam positions are analysed by calculating the Singular Value Decomposition (SVD); finding the major axis between the two data sets returns the scale factor between the XBPM response and the EBPM projections [4]. Figure 2 shows the correlation between the measured and the projected XBPM measurement.

---

* claire.houghton@diamond.ac.uk

A time series plot, Fig. 3, shows the projection of the EBPM measurement in good agreement with the measured XBPM position both horizontally and vertically. The standard deviation of the residual error between the two measurements once the scale factor was applied was 0.29 µm horizontally and 0.30 µm vertically.

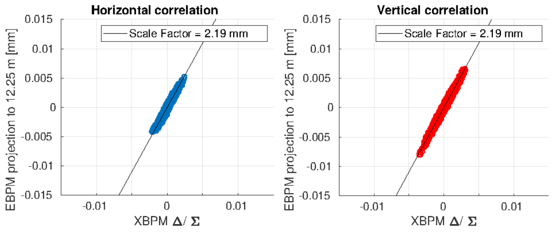

Figure 2: Graphs showing the horizontal (left) and vertical (right) correlation between the projected and measured XBPM position. The scale factor shown here is calculated from the SVD of the correlation.

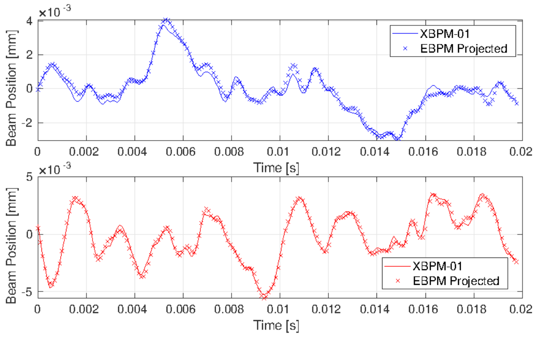

Figure 3: The horizontal (top) and vertical (bottom) beam position over 200 microseconds for the projected EBPM and the measured XBPM with measured scale factor applied.

RESULTS

The scale factors for the XBPM-01 on Diamond Light Source's I14 beamline were measured over a range of ID gaps using the three methods described above. The stepper motor and EBPM angular bump data were collected on the same day and show good agreement with each other over a range of ID gaps as seen in Fig. 4. The non-invasive calibration data shown is the median measured scale factor for each gap acquired using the 1 s long 10 kHz acquisitions collected over a 7-day period. The error bars represent the standard deviation from the measured median. The median of the data was taken in order to minimise the impact of possible outliers on the result (for example particularly noisy measurements acquired immediately after top-up injections; or measurements acquired immediately after an ID gap movement). All three methods show good quantitative agreement over the 5.0 - 9.0 mm range of ID gaps used by the beamline. There is a slightly better correlation in the vertical axis than in the horizontal axis. The reasons for this are not yet fully understood.

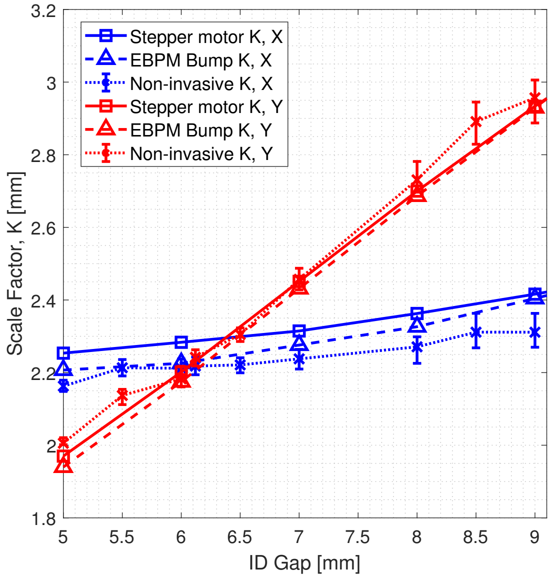

Figure 4: Graph showing the measured scale factors by three calibration methods over a range of ID gaps.

Over the course of a run there are multiple things that can impact the scale factor. These include the machine parameters such as ID gap, as seen in Fig. 4, and environmental factors such as temperature and humidity. Data collected over a 5 week period of user operation has been analysed. Sorting the data by the ID gap, to within 0.5 mm, and taking the median over different time scales it is possible to see how long term machine drifts impact the scale factor. Figure 5 shows the median scale factor for a constant ID gap, 6 mm, over different timescales: 1 week, 24 hours and 1 hour. The error bars represent the standard deviation of the data from the median value at a given ID gap. Over the course of the week both the 24 hour and 1 hour median data shows broadly the same trend for the horizontal and vertical scale factors. The error bars on the three data sets are nominally the same, suggesting that taking the median over a week does not reduce the accuracy in the calibration by a significant amount.

In Fig. 6 the full 5 weeks of measured scale factors is shown, with the median taken over 1 hour periods. The importance of obtaining accurate scale factors at multiple different ID gaps is illustrated by how much the scale factors vary under each of the beamline's different operating conditions and gaps over this period. For example, when the beamline steps the ID gap from 7.0 mm to 8.5 mm increasing K_y by 19%. In addition, similar drifts to those seen in Fig. 5 are present with an increase in K_y on day 20 before returning to the nominal level a few hours later. This change is independent of the ID parameters and would not have been observed using previous methods. Although the mechanism behind this variation in K_y is not understood, it is nonethe-

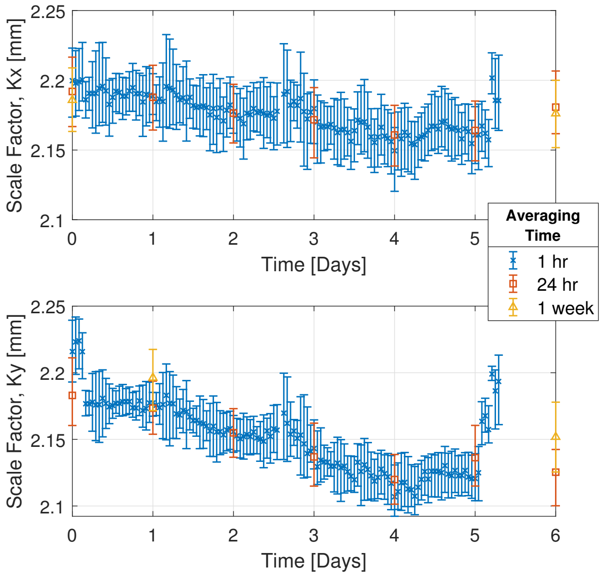

Figure 5: The median scale factor measured over 6 days of data collection using different time-scales for ID gap of 6 mm. The error bars represent the standard deviation from the median. (Top) horizontal K_x, (Bottom) vertical K_y.

less useful information and can help identify potential issues either with the synchrotron or with the XBPMs themselves. The variation in K_y implies that the X-ray beam size may be varying, which could impact the beamline.

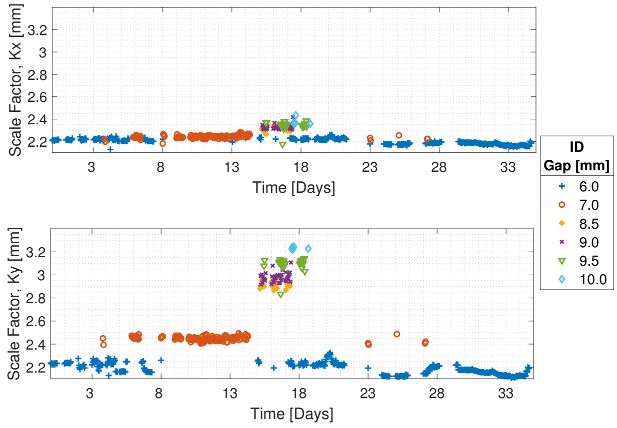

Figure 6: The median scale factors measured over 24 hour periods across 5 weeks of data collection. A range of ID gaps used by the beamline are plotted. (Top) horizontal K_x, (Bottom) vertical K_y.

CONCLUSION

The good agreement between the non-invasive method for calculating calibration factors with previously understood methods, the stepper motor movements and EBPM angular bump, suggest it can be used in place of or alongside those existing methods. There are some discrepancies with the non-invasive method but results show K_x and K_y are equal of previous methods to within 5% and 3% respectively. The reduced time required for collecting data and the ability to obtain more accurate results for the most used gaps could mean the scale factors are more representative of the needs of the users.

By analysing the long term drift of the scale factors the impact of machine drifts can be seen. Currently these calculations are being done offline at the end of the week allowing for corrections to be made in line with machine and environmental drifts. In future these scale factors could be done in real-time and be available as an on-line diagnostic.

FUTURE WORK

Currently the system has been used for data collection and analysis. Applying the measured scale factors and assessing the residual drift is the next step [5]. The causes of the long term drifts seen in Figs. 5 and 6 are not fully understood. The direct comparison between the drifts and measured humidity do not show a clear correlation, suggesting there are other mechanisms involved. Further work is also needed to understand the cause for the discrepancy between the three methods for scale factor calculation described. This method also has a use for calibrating the XBPMs observing beam from Elliptically Polarising Undulators where the beam size and shape can vary significantly depending on the operating mode. Building up calibration tables using stepper motor movements can be time consuming as there are so many potential combinations of ID gap and phase. The technique presented in this paper would enable on-line lookup tables to be generated during normal user operation.

REFERENCES

[1] O. Singh and G. Decker, “Operational Experience with X-ray Beam Position Monitors at the Advanced Photon Source (Invited)”, in *Proc. PAC’01*, Chicago, IL, USA, Jun. 2001, paper ROAB008, pp. 539–543. `https://jacow.org/p01/papers/ROAB008.pdf`

[2] T. Warwick, N. Andresen, G. Portmann and A. Jackson, “Performance of photon position monitors and stability of undulator beams at the advanced light source”, *Rev. Sci. Instrum.*, vol. 66, pp. 1984–1986, `doi:10.1063/1.1145777`

[3] M. G. Abbott, G. Rehm, and I. Uzun, “A New Fast Data Logger and Viewer at Diamond: the FA Archiver”, in *Proc. ICALEPCS’11*, Grenoble, France, Oct. 2011, paper THCHMUST03, pp. 1244–1247.

[4] C. Bloomer and G. Rehm, “Real-time Calculation of Scale Factors of X-ray Beam Position Monitors during User Operation”, in *Proc. IBIC’12*, Tsukuba, Japan, Oct. 2012, paper MOPA13, pp. 79–82.

[5] D. Shu *et al.*, “Smart X-ray beam position monitor system using artificial-intelligence methods for the Advanced Photon Source insertion-device beamlines”, *J. Synchrotron Radiat.*, vol. 5, no. 3, pp. 632–635, May 1998. `doi:10.1107/S0909049597017056`